


 Cite this: *CrystEngComm*, 2015, **17**, 5609

 Received 19th April 2015,
 Accepted 23rd June 2015

DOI: 10.1039/c5ce00762c

www.rsc.org/crystengcomm

Two new porous coordination polymers (PCPs), $[(\text{Cu}_6(\text{L})_4 \cdot (\text{H}_2\text{O})_6] \cdot 10\text{DMA} \cdot 4\text{EtOH}$, (1) and $[\text{Cu}_5(\text{L})_2 \cdot (\text{OH})_2 \cdot (\text{H}_2\text{O})_2 \cdot \text{DMA}_2] \cdot 2\text{DMA} \cdot \text{EtOH} \cdot 2\text{H}_2\text{O}$ (2), were solvothermally synthesized and structurally characterized. Interestingly, their variable architectures controlled by solvent system exhibit a structural progression from an unusual non-crystallographic (NC) net to a (4,6)-connected framework with **fsh** topology. Moreover, the combination of 3D channels of about 3.0×7.2 , 4.7×9.5 , and $6.3 \times 7.8 \text{ \AA}^2$, and functional $-\text{OH}$ groups in 2' lead to good selectivity of CO_2 over CH_4 (26–55 by IAST) at 273 K.

Porous coordination polymers (PCPs), with the tunable nature of their structure and properties, are excellent rivals to other porous materials, such as zeolites and activated carbon, for gas storage and separation.¹ However, the rational control of coordination assemblies remains a challenge.^{1a,g,2} Because, many factors (reactant stoichiometry, temperature, pH, solvent, reaction time and template agents) may affect the final architectures.³ Among them, solvent systems have been found to produce more dramatic effects on self-assembly.⁴ This is because, by acting as a template or a second ligand, the traditional coordination geometry that is preferred by the metal center could be changed.⁵ The generated structure cannot follow the rules of reticular chemistry, even based on well-designed ligands. Thus, further investigation of solvent systems in the formation of coordination polymers is very essential.

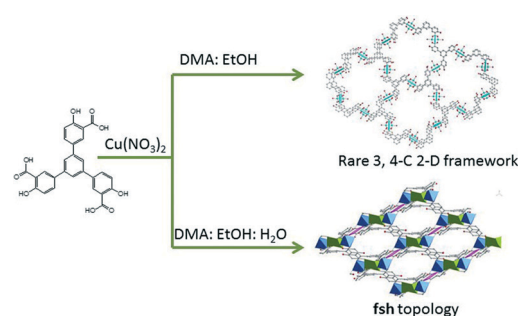
In addition, exposed functional sites and an optimized pore size play important roles in selective gas capture, due to

Two solvent-dependent porous coordination polymers with $-\text{OH}$ decorated ligands: unusual non-crystallographic net and **fsh** topology†

 Jingui Duan,^{*a} Masakazu Higuchi,^{bc} Changchang Zou,^a Wanqin Jin^a and Susumu Kitagawa^b

the enhanced ability of host–guest interactions and also maximum size exclusion effects.⁶ The immobilization of functional sites (such as open metal sites and alkylamines) into PCPs was considered as rational design.⁷ Moreover, by introducing some specific substituent groups, *e.g.* $-\text{NH}_2$, $-\text{COOH}$ on the pore surface also worked well.⁸ However, there is a dearth of research on the investigation of the impact of open $-\text{OH}$ groups in PCPs, because of the difficulty of getting open $-\text{OH}$ sites after coordination assembly.⁹

We are interested in the design and construction of porous coordination polymers with functional pores for the recognition of energy gas molecules, and identifying a series of water and chemical stable frameworks for expected feasible gas storage and separation.¹⁰ Here, continuing our work, we report the syntheses of two new PCPs, $[(\text{Cu}_6(\text{L})_4 \cdot (\text{H}_2\text{O})_6] \cdot 10\text{DMA} \cdot 4\text{EtOH}$, (1, the desolvated solid is named as 1'), and $[\text{Cu}_5(\text{L})_2 \cdot (\text{OH})_2 \cdot (\text{H}_2\text{O})_2 \cdot \text{DMA}_2] \cdot 2\text{DMA} \cdot \text{EtOH} \cdot 2\text{H}_2\text{O}$ (2, the desolvated solid is named as 2'), ($\text{H}_6\text{L} = 1,3,5\text{-tris}(3\text{-carboxy-4-hydroxylphenyl})\text{benzene}$), based upon a ligand with an $-\text{OH}$ functional group. Interestingly, their variable architectures controlled by solvent system exhibit a structural progression from an unusual NC net to a (4,6)-connected framework with **fsh** topology. In addition, PCP 2 bearing a suitable pore size, as well as an open $-\text{OH}$ site shows high selectivity of CO_2 over CH_4 (25–55) at 273 K (Scheme 1).



Scheme 1 Synthetic procedures of PCP 1 and 2.

A solvothermal reaction of H_6L and $\text{Cu}(\text{NO}_3)_2 \cdot 6\text{H}_2\text{O}$ in DMA/EtOH afforded green crystals of $[(\text{Cu}_6(\text{L})_4 \cdot (\text{H}_2\text{O})_6) \cdot 10\text{DMA} \cdot 4\text{EtOH}]$. The phase purity of them was confirmed by comparing their experimental powder X-ray diffraction pattern to that calculated based on the single-crystal structures. X-ray diffraction analysis reveals that the L^{3-} ligand in **1** is connected by three copper paddlewheels, and each cluster is bridged by four carboxylate groups from four different ligands, forming a highly symmetrical fan-like sub-structure (Fig. 1). The double layers of fan-like structures share their edges with each other to generate a 1D channel with a diameter of 15.6 \AA . In addition, all of the inserted $-\text{OH}$ groups are well-aligned inside the channels of **1** (Fig. 1d). For the easy understanding of the connection of this structure, we simply assign the $\text{Cu}_2(\text{ArCOO})_4$ units as 4-connected nodes, and L^{3-} units as 3-connected linkers. The 3-c nodes come in pairs in which each of them is connected to the same three 4-c nodes. Clearly there is a net automorphism that simply involves interchanging those two vertices, leaving the rest fixed.¹¹ Thus, the generated topology of **1** is an example of a non-crystallographic (NC) net that is different to the another two (3,4)-connected nets of HKUST-1(tbo)¹² and MOF-14 (pto).¹³ This significant change can be explained as being due to the shift of the coordination site from the 4- to 3-position of the benzene ring. The total accessible volume of desolvated **1** is *ca.* 71.1%, calculated using the PLATON program.¹⁴ Additionally, the powder X-ray diffraction (PXRD) pattern showed that the peak positions of the as-synthesized phase are the same

as the simulated data, but the peak intensity, especially for the $[2\ 0\ 0]$ peak, is different. This is because **1** exhibits a stronger preferential orientation along the $[2\ 0\ 0]$ direction.¹⁵ Meanwhile, with very good reliability factors ($R_p = 0.0252$ and $R_{wp} = 0.0553$), Le Bail analysis of the PXRD pattern shows that the refined parameters are very close to the data from the single crystal, reflecting good phase purity and also a well-defined structure (Fig. S8†).

$[\text{Cu}_5(\text{L})_2(\text{OH})_2 \cdot (\text{H}_2\text{O})_2 \cdot \text{DMA}_2] \cdot 2\text{DMA} \cdot \text{EtOH} \cdot 2\text{H}_2\text{O}$ (**2**) was harvested from a DMA/EtOH/ H_2O solvent system. Interestingly, crystallographic analysis revealed that **2** crystallizes in $P\bar{1}$ space group (Fig. 2). The asymmetric unit of **2** includes one half $\text{Cu}(\text{II})$ atom (Cu1) on an inversion centre, two other $\text{Cu}(\text{II})$ atoms in general positions, one partially deprotonated L ligand, one $-\text{OH}$ group, one coordinated water molecule and one coordinated DMA molecule (Fig. 2a). The coordination numbers of these three copper atoms are 4, 5 and 5, respectively. The coordination geometry of Cu1 is a slightly distorted pentahedron, and is completed by two oxygen atoms from bridged $-\text{OH}$ groups, two oxygen atoms from the carboxylate groups, and one coordinated water molecule. Meanwhile, the coordination geometry of Cu2 is completed by one oxygen atom from a bridged $-\text{OH}$ group, three oxygen atoms from the carboxylate groups, and one coordinated DMA molecule. Last but not least, a rare and planar coordination square around Cu3 is finished by two phenols oxygen atoms and two carboxylate oxygen atoms. In addition, one ligand is connected by five Cu atoms, forming a porous 3D framework. Thus, a high

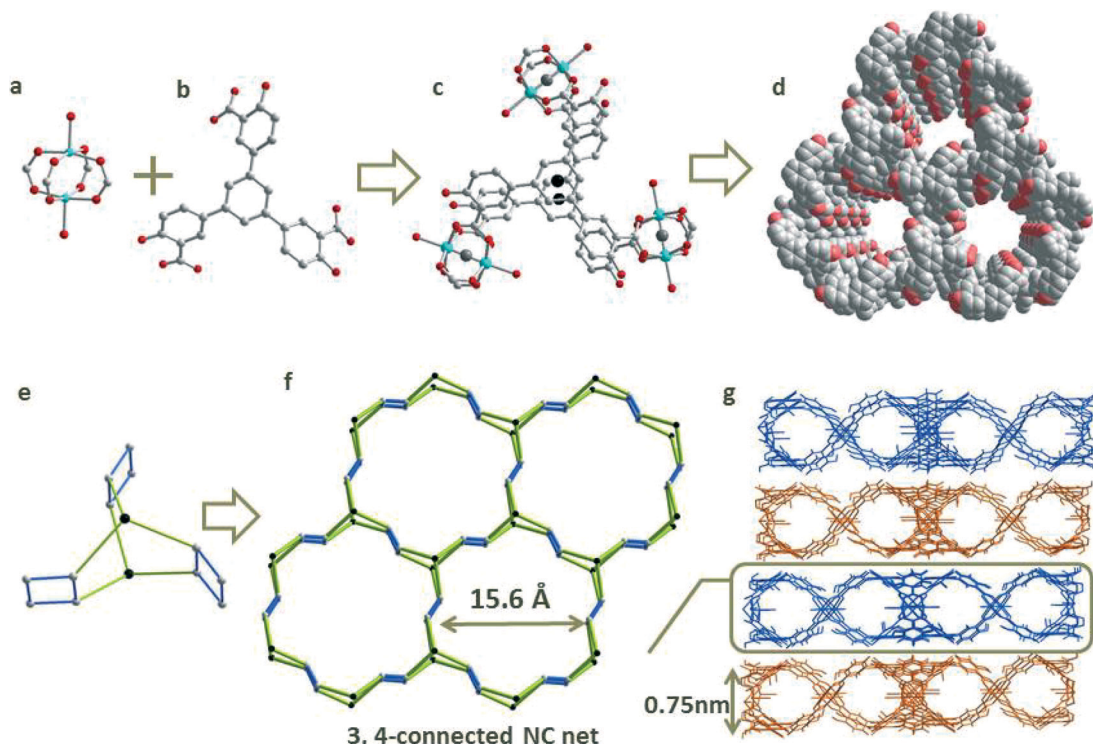


Fig. 1 The structure of **1**: (a) the dicopper cluster; (b) H_6L ligand; (c) double layered fan-like structure; (d) functional and free $-\text{OH}$ groups aligned inside the 1D channel (O atoms from the $-\text{OH}$ groups are highlighted in a red color); (e) the simplification method; (f) unusual 3,4-connected NC net; (g) the packing of the 2D framework with a 0.75 nm layer height.

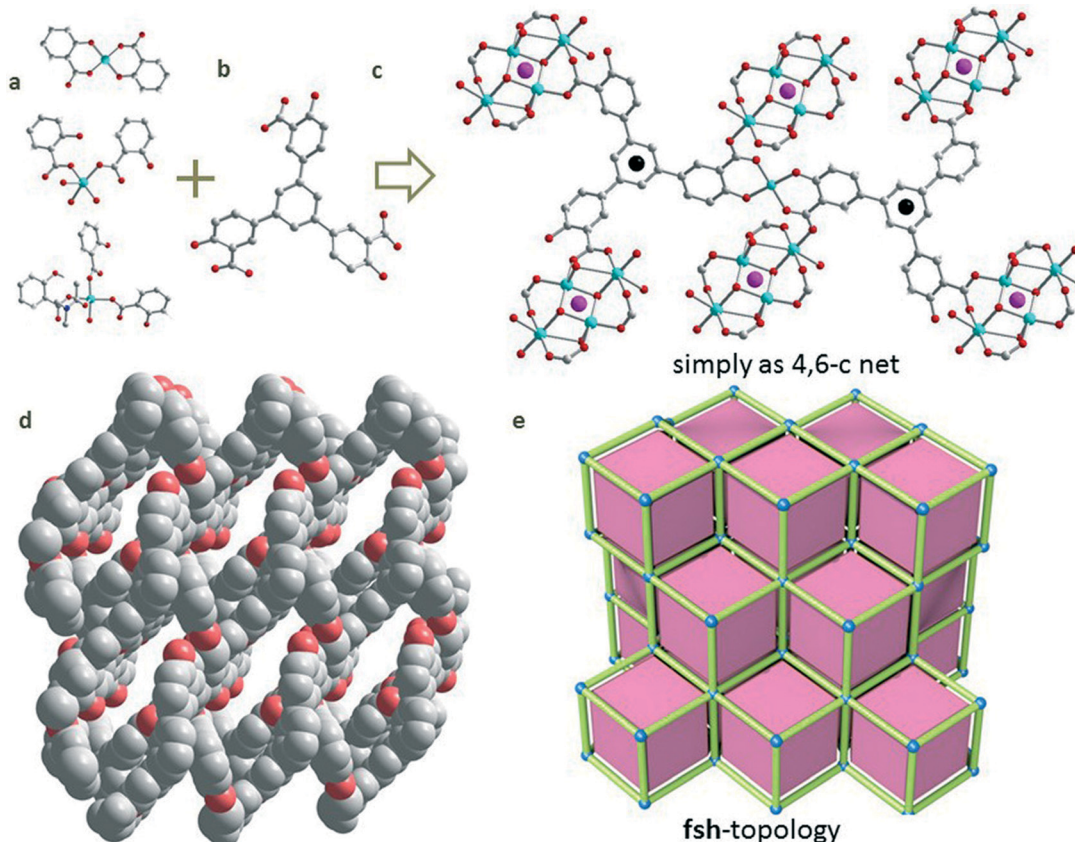


Fig. 2 The structure of 2: (a) the three different coordination geometries of the Cu²⁺ atoms; (b) the H₆L ligand; (c) the simple method; (d) functional -OH groups aligned inside the 1-D channel (O atoms from -OH groups are highlighted in red); (e) fsh topology with one kind of tiling.

density of open metal sites can be expected in 2, due to the existence of the original open metal site and also the sites from the removal of coordinated DMA and water. In addition, free -OH groups can also be found inside the channel as shown in Fig. 2d. Compared with the significant channel in 1, the structure of 2 with 3D intercrossed channels of about 3.0 × 7.21, 4.72 × 9.52, and 6.37 × 7.81 Å² indicates a suitable pore size for CO₂ separation (kinetic parameter of CO₂: 3.3 Å). The total accessible volume of desolvated 2 is *ca.* 41.5%, calculated using the PLATON program.¹⁴ In addition, after soaking 2 in water for 1 day, the PXRD profiles show the integrity of the framework (Fig. S9†), which is a rare result for carboxylate- and Cu-based PCPs. In order to further understand the connection of 2, the Cu₄(ArCOO)₄(OH)₂ and Cu(ArCOO)₂(ArO)₂ clusters were simplified as 4- and 2-connected nodes, where the L⁴⁻ ligands are 4-connected linkers (Fig. 2c). However, it is usual to subsume 2-connected vertices into a link, and then the generated basic unit of 2 can be assigned as a hexatopic carboxylate linker that joins 4-connected nodes. Considering the 4-c branch points of the L⁴⁻ unit, the framework shows a (4,6)-c net with fsh topology (Fig. 2e).

Interestingly, comparing the synthesis conditions of these two PCPs (changing the solvent systems, while the other conditions were intentionally held constant), we found that the

solvent systems induced the changed coordination of the ligand, as well as the structural progression. In order to confirm this point, the following experiments were conducted and the observations from PXRD (Fig S7 and S11†) are detailed in Table 1: (1) when DMA/EtOH (2 mL, 4:2) is used as a solvent system, 1 with phase purity can be obtained at 65 °C, but not at 90 °C and 130 °C; (2) when a very small amount of water was added to the DMA/EtOH system (2 mL, DMA:EtOH:H₂O = 4:2:0.5), we got purified 2 at 65 °C; (3) when we increased the amount of water in the solvent system from 4:2:0.5 to 4:2:2, only 2 could be generated at 65 and 90 °C and (4) when the amount of water increased to a very high level (4:2:12), no PCPs could be formed at the three temperatures. Thus, different solvent systems regulate the formation of different environments for the assembly of Cu(II) and the linking modes of the H₆L ligand. In 1, only the

Table 1 Experimental matrix of PCP syntheses

Temperature, time and solvent	DMA:EtOH:H ₂ O			
	4:2:0	4:2:0.5	4:2:2	4:2:12
65 °C, 48 h	1	2	2	×
90 °C, 48 h	×	×	2	×
130 °C, 48 h	×	×	×	×

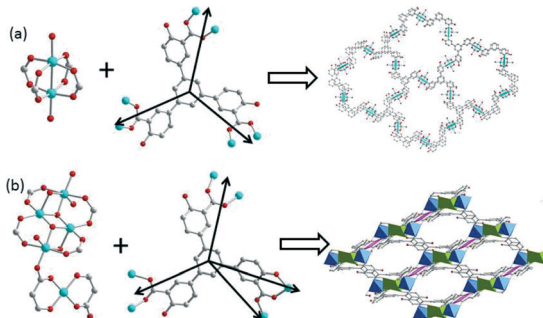


Fig. 3 The coordination of metals and ligands in PCP 1 (a) and 2 (b).

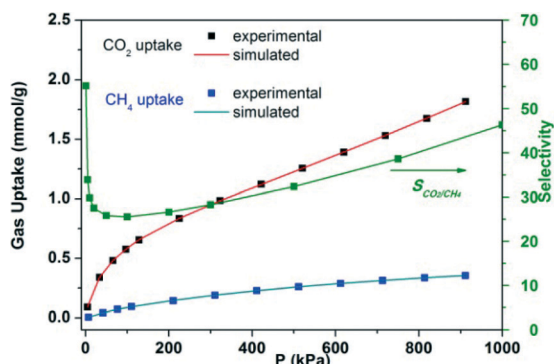


Fig. 4 High pressure gas adsorption isotherms and the Dual-site Langmuir-Freundlich fit lines of CO₂ and CH₄ in 2' at 273 K. The green lines show the IAST predicted selectivity of CO₂ over CH₄.

carboxylate groups coordinated to the Cu(II) paddlewheel nodes, whereas, in 2, three different coordination geometries were bridged by the carboxylate groups and also an -OH group from the ligand. Therefore, the ligand can be simplified as three- and four-connected linkers in 1 and 2, respectively. Then, a structural progression from an unusual NC net to a (4,6)-connected framework with fsh topology was well observed (Fig. 3). Herein, more theoretical and experimental efforts are required for finding the role of water in influencing the coordination self-assembly, but we can make a preliminary conclusion: the volumetric ratio of water in a mixed solvent system may influence the solvation process and coordination kinetics in solution. This is maybe due to water being a kind of special ligand that can result in a new balance of the kinetics and thermodynamics of the final product.^{4,16}

Encouraged by the porous and functional sites in the PCPs, the gas adsorption of them was measured. Before the gas sorption experiments, the activation of these two structures was explored. Unfortunately, desolvated 1' collapsed, and did not show any gas uptake. Meanwhile, compound 2' showed a little CO₂ gas uptake (25 cm³ g⁻¹) at 1 bar and 195 K. The PXRD pattern of desolvated 2' indicated structural change after the activation. However, interestingly, 2' did not show any uptake of O₂, CH₄, C₂H₄ and C₂H₆ (Fig. S14[†]). Thus, the unique gas adsorption isotherms show the

possibility of the selective capture of CO₂ by 2'. The adsorption isotherms of CO₂ and CH₄ in 2' were collected at 273 K to 9 bar. The maximum uptakes of them reached 1.82 mmol g⁻¹ and 0.35 mmol g⁻¹, respectively. In order to explore the selectivity of 2', ideal adsorbed solution theory was employed to predict multi-component adsorption behaviors from the experimental pure-gas isotherms. The predicted adsorption selectivity for equimolar CO₂/CH₄ mixtures in 2' as a function of bulk pressure is presented in Fig. 4. The selectivity of CO₂ over CH₄ is very sensitive to loading and shows two steps in the changes of selectivity: a quick decrease of CO₂ selectivity in the low pressure region, and a slow increase at high pressure (22–55). This high selectivity can be explained as a result of the good combination of suitable pore size, open metal sites and functionalized -OH groups in 2'. In addition, based on the IAST model and similar conditions, these selectivities are higher than those of the reported adsorbent materials (Zn₂(NDC)₂(DPNI)) (30),¹⁷ Zn₅(BTA)₆(TDA)₂ (37),¹⁸ Cu-BTC (6–10),¹⁹ zeolites 13× (2–24)²⁰ and comparable with the performance of our previously reported amide-functionalized materials of NJU-Bai3 (25–60),^{10b} indicating a selective removal of CO₂ from natural gas.

Conclusions

In summary, we have demonstrated the water-controlled assembly of two new porous coordination polymers originating from the variable coordination of the ligands around the metal center. Interestingly, their variable architectures controlled by solvent systems exhibit a structural progression from an unusual non-crystallographic net to a (4,6)-connected 3D framework with fsh topology. PCP 2, possessing a suitable pore size and functional -OH groups, exhibits good gas selectivity of CO₂ (S_{CO₂/CH₄}: 22–55). Therefore, we believe that our results could further the perspective of the chemistry of structural control and progression in the area of PCPs.

Acknowledgements

The authors gratefully acknowledge support from the Natural Science Foundation of China (no. 21301148), Talent Development Program of Nanjing Tech University (39801116), Advanced Catalytic Transformation Program for Carbon Utilization (ACT-C), the PRESTO Program of the Japan Science and Technology Agency (JST), ENEOS Hydrogen Trust Fund. The Institute for Integrated Cell-Material Sciences (iCeMS) is supported by the World Premier International Research Initiative (WPI). We thank Dr. Mawlin Foo for discussion.

Notes and references

- (a) S. Kitagawa, R. Kitaura and S. Noro, *Angew. Chem., Int. Ed.*, 2004, 43, 2334–2375; (b) R. Matsuda, R. Kitaura, S. Kitagawa, Y. Kubota, R. V. Belosludov, T. C. Kobayashi, H. Sakamoto, T. Chiba, M. Takata, Y. Kawazoe and Y. Mita, *Nature*, 2005, 436, 238–241; (c) H. Furukawa, N. Ko, Y. B. Go, N. Aratani, S. B. Choi, E. Choi, A. O. Yazaydin, R. Q. Snurr,

- M. O'Keeffe, J. Kim and O. M. Yaghi, *Science*, 2010, **329**, 424–428; (d) O. K. Farha, A. O. Yazaydin, I. Eryazici, C. D. Malliakas, B. G. Hauser, M. G. Kanatzidis, S. T. Nguyen, R. Q. Snurr and J. T. Hupp, *Nat. Chem.*, 2010, **2**, 944–948; (e) D. Q. Yuan, D. Zhao, D. F. Sun and H. C. Zhou, *Angew. Chem., Int. Ed.*, 2010, **49**, 5357–5361; (f) L. Ma, C. Abney and W. Lin, *Chem. Soc. Rev.*, 2009, **38**, 1248–1256; (g) J. P. Zhang, Y. B. Zhang, J. B. Lin and X. M. Chen, *Chem. Rev.*, 2012, **112**, 1001–1033; (h) H. L. Jiang and Q. Xu, *Chem. Commun.*, 2011, **47**, 3351–3370; (i) M. Hirscher, *Angew. Chem. Int. Ed.*, 2011, **50**, 581–582; (j) R. Vaidhyanathan, S. S. Iremonger, G. K. H. Shimizu, P. G. Boyd, S. Alavi and T. K. Woo, *Science*, 2010, **330**, 650–653.
- 2 (a) G. Ferey, C. Mellot-Draznieks, C. Serre and F. Millange, *Acc. Chem. Res.*, 2005, **38**, 217–225; (b) B. Moulton and M. J. Zaworotko, *Chem. Rev.*, 2001, **101**, 1629–1658.
- 3 (a) Y. T. Wang, H. H. Fan, H. Z. Wang and X. M. Chen, *Inorg. Chem.*, 2005, **44**, 4148–4150; (b) J. G. Duan, B. S. Zheng, J. F. Bai, Q. A. Zhang and C. Y. Zuo, *Inorg. Chim. Acta*, 2010, **363**, 3172–3177; (c) L. Carlucci, G. Ciani, D. M. Proserpio and S. Rizzato, *New J. Chem.*, 2003, **27**, 483–489; (d) B. Zheng, J. F. Bai and Z. X. Zhang, *CrystEngComm*, 2010, **12**, 49–51; (e) D. M. Shin, I. S. Lee, D. Cho and Y. K. Chung, *Inorg. Chem.*, 2003, **42**, 7722–7724; (f) B. Zheng, H. Dong, J. F. Bai, Y. Z. Li, S. H. Li and M. Scheer, *J. Am. Chem. Soc.*, 2008, **130**, 7778–7779.
- 4 P. P. Cui, J. L. Wu, X. L. Zhao, D. Sun, L. L. Zhang, J. Guo and D. F. Sun, *Cryst. Growth Des.*, 2011, **11**, 5182–5187.
- 5 I. S. Lee, D. M. Shin and Y. K. Chung, *Chem. – Eur. J.*, 2004, **10**, 3158–3165.
- 6 (a) J. R. Li, Y. G. Ma, M. C. McCarthy, J. Sculley, J. M. Yu, H. K. Jeong, P. B. Balbuena and H. C. Zhou, *Coord. Chem. Rev.*, 2011, **255**, 1791–1823; (b) D. M. D'Alessandro, B. Smit and J. R. Long, *Angew. Chem., Int. Ed.*, 2010, **49**, 6058–6082.
- 7 (a) D. Britt, H. Furukawa, B. Wang, T. G. Glover and O. M. Yaghi, *Proc. Natl. Acad. Sci. U. S. A.*, 2009, **106**, 20637–20640; (b) A. Demessence, D. M. D'Alessandro, M. L. Foo and J. R. Long, *J. Am. Chem. Soc.*, 2009, **131**, 8784–8785.
- 8 A. Torrisi, R. G. Bell and C. Mellot-Draznieks, *Cryst. Growth Des.*, 2010, **10**, 2839–2841.
- 9 (a) H. X. Deng, S. Grunder, K. E. Cordova, C. Valente, H. Furukawa, M. Hmadeh, F. Gandara, A. C. Whalley, Z. Liu, S. Asahina, H. Kazumori, M. O'Keeffe, O. Terasaki, J. F. Stoddart and O. M. Yaghi, *Science*, 2012, **336**, 1018–1023; (b) Z. X. Chen, S. C. Xiang, H. D. Arman, P. Li, D. Y. Zhao and B. L. Chen, *Eur. J. Inorg. Chem.*, 2011, 2227–2231.
- 10 (a) J. G. Duan, M. Higuchi, S. Horike, M. L. Foo, K. P. Rao, Y. Inubushi, T. Fukushima and S. Kitagawa, *Adv. Funct. Mater.*, 2013, **23**, 3525–3530; (b) J. G. Duan, Z. Yang, J. F. Bai, B. S. Zheng, Y. Z. Li and S. H. Li, *Chem. Commun.*, 2012, **48**, 3058–3060; (c) J. G. Duan, M. Higuchi, R. Krishna, T. Kiyonaga, Y. Tsutsumi, Y. Sato, Y. Kubota, M. Takata and S. Kitagawa, *Chem. Sci.*, 2014, **5**, 660–666; (d) B. S. Zheng, J. F. Bai, J. G. Duan, L. Wojtas and M. J. Zaworotko, *J. Am. Chem. Soc.*, 2011, **133**, 748–751; (e) J. G. Duan, W. Q. Jin and R. Krishna, *Inorg. Chem.*, 2015, **54**, 4279–4284; (f) J. G. Duan, M. Higuchi and S. Kitagawa, *Inorg. Chem.*, 2015, **54**, 1645–1649.
- 11 O. Delgado-Friedrichs, S. T. Hyde, S. W. Mun, M. O'Keeffe and D. M. Proserpio, *Acta Crystallogr., Sect. A: Found. Crystallogr.*, 2013, **69**, 535–542.
- 12 S. S. Y. Chui, S. M. F. Lo, J. P. H. Charmant, A. G. Orpen and I. D. Williams, *Science*, 1999, **283**, 1148–1150.
- 13 B. L. Chen, M. Eddaoudi, S. T. Hyde, M. O'Keeffe and O. M. Yaghi, *Science*, 2001, **291**, 1021–1023.
- 14 A. L. Spek, *PLATON, A Multipurpose Crystallographic Tool*, Utrecht University, 2001.
- 15 K. Rao, M. Higuchi, K. Sumida, S. Furukawa, J. Duan and S. Kitagawa, *Angew. Chem., Int. Ed.*, 2014, **53**, 8225–8230.
- 16 (a) S. R. Caskey, A. G. Wong-Foy and A. J. Matzger, *Inorg. Chem.*, 2008, **47**, 7751–7756; (b) D. Frahm, F. Hoffmann and M. Froba, *Cryst. Growth Des.*, 2014, **14**, 1719–1725; (c) Y. Wang, S. X. Cui, B. Li, J. P. Zhang and Y. Zhang, *Cryst. Growth Des.*, 2009, **9**, 3855–3858.
- 17 Y. S. Bae, K. L. Mulfort, H. Frost, P. Ryan, S. Punnathanam, L. J. Broadbelt, J. T. Hupp and R. Q. Snurr, *Langmuir*, 2008, **24**, 8592–8598.
- 18 Z. J. Zhang, S. C. Xiang, Y. S. Chen, S. Q. Ma, Y. Lee, T. Phely-Bobin and B. L. Chen, *Inorg. Chem.*, 2010, **49**, 8444–8448.
- 19 Q. Y. Yang and C. L. Zhong, *J. Phys. Chem. B*, 2006, **110**, 17776–17783.
- 20 S. Cavenati, C. A. Grande and A. E. Rodrigues, *J. Chem. Eng. Data*, 2004, **49**, 1095–1101.